# High-Accuracy Finite Element Method for the 2D Parametric Elliptic Boundary-Value Problems

S.I. Vinitsky (JINR, Dubna)

A.A. Gusev,
O. Chuluunbaatar,
G. Chuluunbaatar,
(JINR)

06 July 2017

International Conference
"Mathematical Modeling and
Computational Physics'

OUTLINE

- The statement of the problem
- Lagrange Finite Elements
- Example of parametric 2D BVP for a Helium atom
- Resume

# The statement of the problem

## A self-adjoint elliptic PDE in the region $z = (z_1, ..., z_d) \in \Omega \subset \mathcal{R}^d$ ($\Omega$ is polyhedra)

$$\left( -\frac{1}{g_0(z)} \sum_{ij=1}^{d} \frac{\partial}{\partial z_i} g_{ij}(z) \frac{\partial}{\partial z_j} + V(z) - E \right) \Phi(z) = 0,$$

$g_0(z) > 0$, $g_{ji}(z) = g_{ij}(z)$ and $V(z)$ are the real-valued functions, continuous together with their generalized derivatives to a given order.

## The Dirichlet (I) and Neumann (II) boundary conditions

$$(I) : \Phi(z)|_S = 0, \qquad (II) : \left.\frac{\partial \Phi(z)}{\partial n_D}\right|_S = 0, \quad \frac{\partial \Phi(z)}{\partial n_D} = \sum_{ij=1}^{d} (\hat{n}, \hat{e}_i) g_{ij}(z) \frac{\partial \Phi(z)}{\partial z_j}.$$

$\frac{\partial \Phi_m(z)}{\partial n_D}$ is the derivative along the conormal direction
$\hat{n}$ is the outer normal to the boundary of the domain $\partial\Omega$.

О.А. Ладыженская, Краевые задачи математической физики (М., Наука, 1973)
В.В. Шайдуров, Многосеточные методы конечных элементов. (М., Наука, 1989).

# The statement of the problem

For a discrete spectrum problem the functions $\Phi_m(z)$ from the Sobolev space $H_2^{s\geq 1}(\Omega)$, $\Phi_m(z) \in H_2^{s\geq 1}(\Omega)$, corresponding to the real eigenvalues $E$: $E_1 \leq E_2 \leq ... \leq E_m \leq ...$ satisfy the conditions of normalization and orthogonality

$$\langle \Phi_m(z) | \Phi_{m'}(z) \rangle = \int\limits_{\Omega} dz g_0(z) \Phi_m(z) \Phi_{m'}(z) = \delta_{mm'}, \quad dz = dz_1 ... dz_d.$$

The FEM solution of the BVP is reduced to the determination of stationary points of the variational functional

$$\Xi(\Phi_m, E_m, z) \equiv \int\limits_{\Omega} dz g_0(z) \Phi_m(z) \left(D - E_m\right) \Phi(z) = \Pi(\Phi_m, E_m, z),$$

$$\Pi(\Phi_m, E_m, z) = \int\limits_{\Omega} dz \left[ \sum_{ij=1}^{d} g_{ij}(z) \frac{\partial \Phi_m(z)}{\partial z_i} \frac{\partial \Phi_m(z)}{\partial z_j} + g_0(z) \Phi_m(z) (V(z) - E_m) \Phi_m(z) \right].$$

Strang, G., Fix, G.J.: An Analysis of the Finite Element Method, Prentice-Hall, Englewood Cliffs, New York (1973)

# Lagrange Finite Elements

The piecewise polynomial functions $N_I(z)$ are constructed by joining the shape functions $\varphi_I(z)$ in the triangle $\Delta_q$:

$$N_I(z) = \left\{ \varphi_I(z), A_I \in \Delta_q; 0, A_I \notin \Delta_q \right\}$$

and possess the following properties:
functions $N_I(z)$ are continuous in the domain $\Omega$;
the functions $N_I(z)$ equal 1 in one of the points $A_I$ and zero in the rest points.

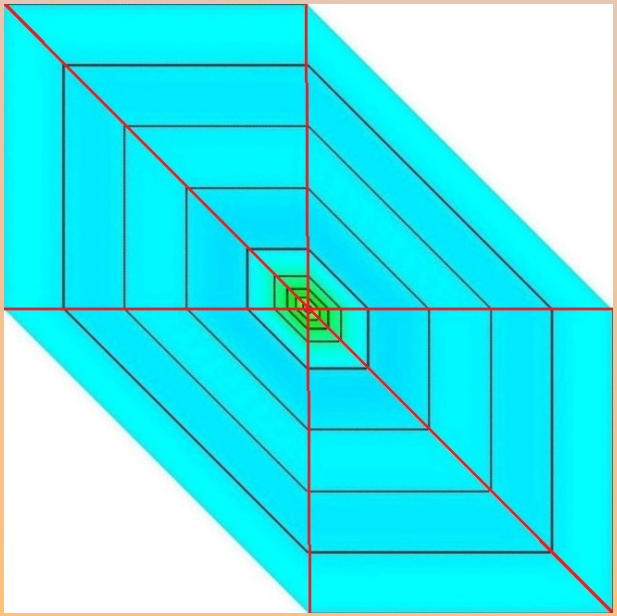
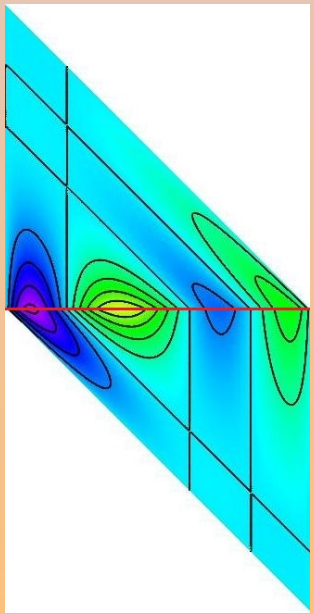
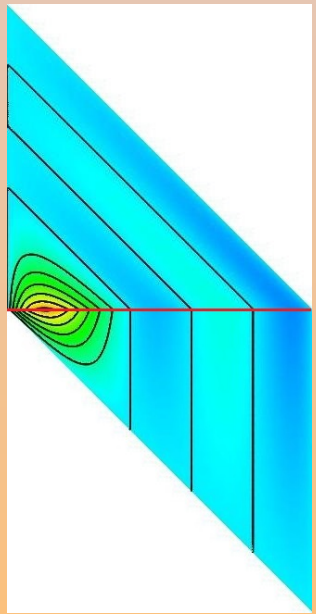
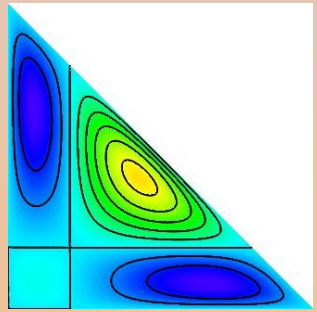
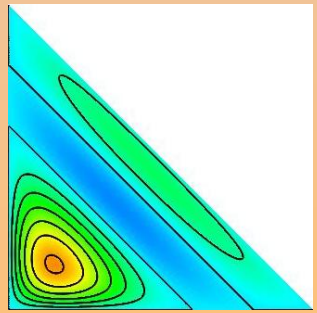

# Finite Element Method

Solutions $\hat{\Phi}(z)$ are sought in the form of a finite sum over the basis of local functions $N_\mu^g(z)$ in each nodal point $z = z_k$ of the grid $\Omega_h(z)$:

$$\hat{\Phi}(z) = \sum_{\mu=0}^{L-1} \Phi_\mu^h N_\mu^g(z),$$

where $L$ is number of local functions, and $\Phi_\mu^h$ are nodal values of function $\hat{\Phi}(z)$ at nodal points $z_l$.

After substituting the expansion into the variational functional and minimizing it, we obtain the generalized eigenvalue problem

$$\mathbf{A}^p \boldsymbol{\xi}^h = \varepsilon^h \mathbf{B}^p \boldsymbol{\xi}^h.$$

Here $\mathbf{A}^p$ is the stiffness matrix; $\mathbf{B}^p$ is the positive definite mass matrix; $\boldsymbol{\xi}^h$ is the vector approximating the solution on the finite-element grid; and $\varepsilon^h$ is the corresponding eigenvalue.

# Decomposition of a hypercube by means of simplexes

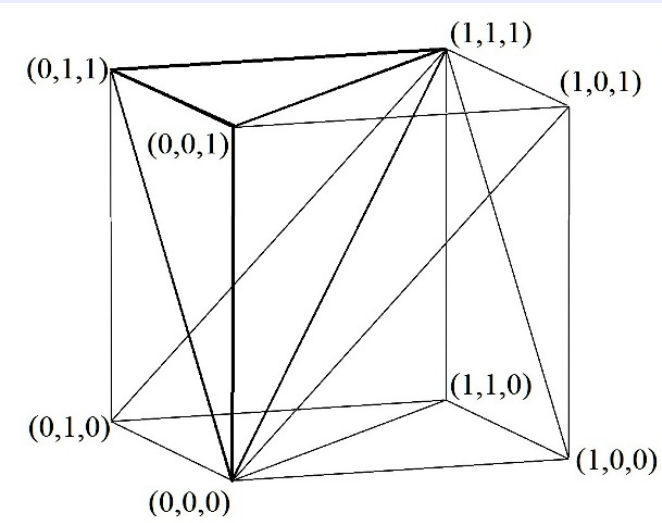


| T1 | T2 |
|---|---|
| (0,0,0) | (0,0,0) |
| (0,0,1) | (0,0,1) |
| (0,1,1) | (1,0,1) |
| (1,1,1) | (1,1,1) |
| **T3** | **T4** |
| (0,0,0) | (0,0,0) |
| (0,1,0) | (0,1,0) |
| (0,1,1) | (1,1,0) |
| (1,1,1) | (1,1,1) |
| **T5** | **T6** |
| (0,0,0) | (0,0,0) |
| (1,0,0) | (1,0,0) |
| (1,0,1) | (1,1,0) |
| (1,1,1) | (1,1,1) |

Assertion. The $d$-dimensional hypercube is divided into $d!$ equal $d$-dimensional simplexes.
The vertices of each of the simplex are located on broken lines, Composed of $d$ mutually perpendicular edges, and the extreme vertices of all polygons are located on one of the diagonals of the hypercube.

## Algorithm.

Input: A single $d$-dimensional hypercube with vertices whose coordinates are either 0 or 1 in the Euclidean space $\mathbf{R}^d$.
The chosen diagonal of the hypercube connects the vertices with the coordinates $(0, ..., 0)$ and $(1, ..., 1)$.
Output. $z_k^{(i)} = (z_{k,1}^{(i)}, ..., z_{k,d}^{(i)})$ the coordinates of $i$-th simplex
Local. The coordinates of the vertices of the polygonal line are $z_k = (z_{k,1}, ..., z_{k,d})$, $k = 0, ..., d$.

For all $i = (i_1, ..., i_d)$, the permutations of the numbers $(1, ..., d)$:
For all $k = 0, ..., d$ and $s = 1, ..., d$:

$$z_{k,s}^{(i)} = \begin{cases} 1, & i_s \le k, \\ 0, & i_s > k. \end{cases}$$

if $\det(z_{k,s}^{(i)})_{k,s=1}^{d} = -1$ then $z_{k,d}^{(i)} \leftrightarrow z_{k,d-1}^{(i)}$.

# Structures of matrices

## 2D

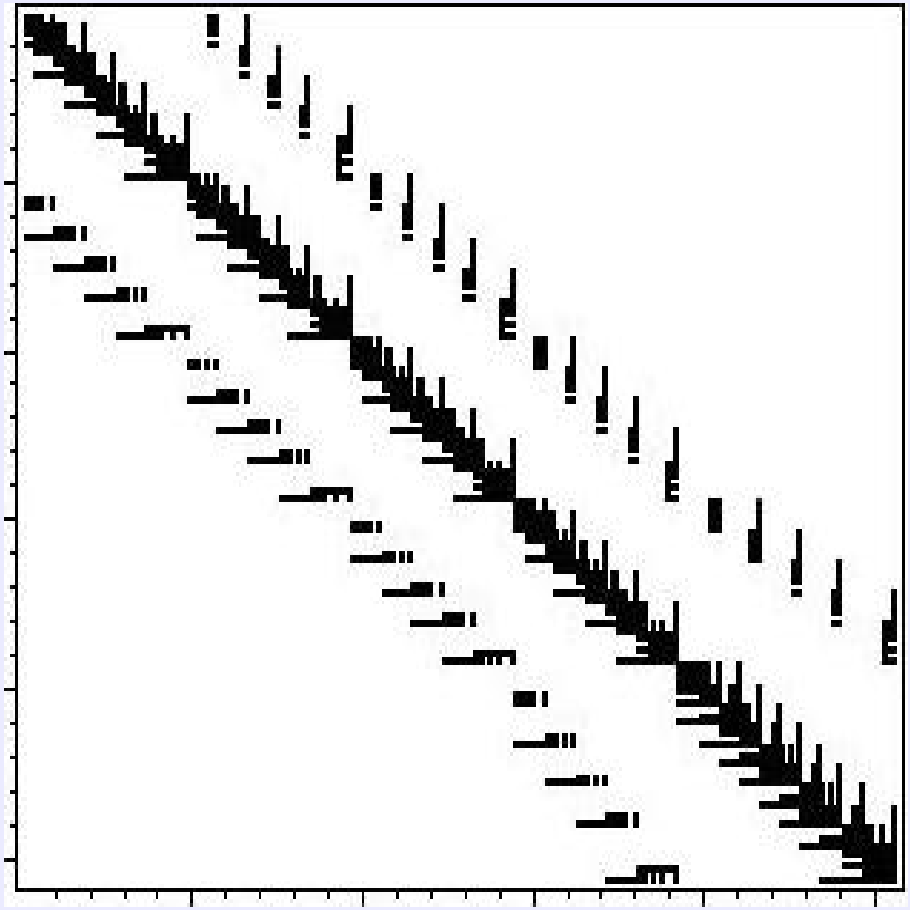

## 3D

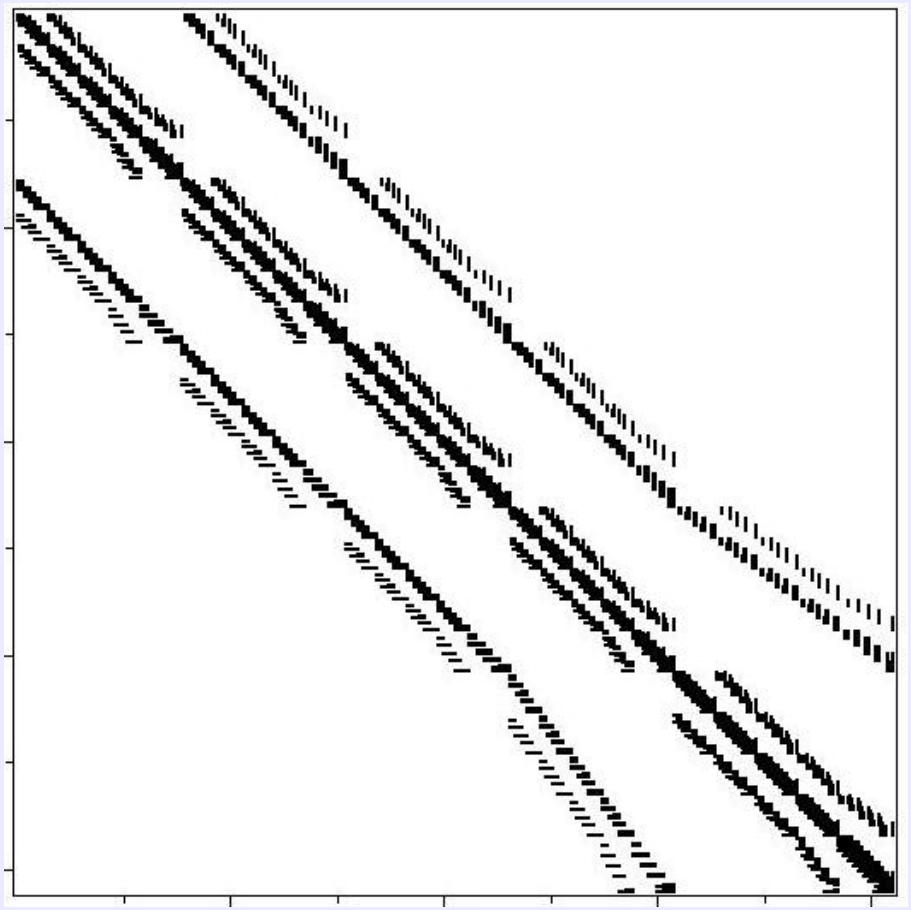

# Example: the BVP for 3D Helmholtz Eq. for the cube with rip equal to $\pi$

The solution of the 3D BVP with Neumann BCs using 3D LIPs of $p = p' =$6th order. Cube with rip $\pi$ divided by $4^3$ cubes each of them composed by 6 tetrahedrons. The matrices $A$ and $B$ had dimension $15625 \times 15625$. Calculations was performed in Maple 2x 8-core Xeon E5-2667 v2 3.3 GHz, 512 GB RAM, GPU Tesla 2075. The matrices $A$ and $B$ were calculated during 14 hours, on Maple, and AEP was solved on Intel Fortran during 20 minutes.

| | E(F) | E(M) | E(F)-E(M) |
|---|---|---|---|
| 1 | 6.E-0030 | 1.7(-12) | 1.7(-12) |
| 2 | 1.0000000000000051 | 0.9999999997 | 0.0000000003 |
| 3 | 1.0000000000000063 | 0.9999999997 | 0.0000000003 |
| 4 | 1.0000000000000063 | 0.9999999997 | 0.0000000003 |
| 5 | 2.0000000000072494 | 2.0000000006 | 0.0000000006 |
| 6 | 2.0000000000072494 | 2.0000000015 | 0.0000000015 |
| 7 | 2.0000000000079230 | 2.0000000017 | 0.0000000017 |
| 8 | 3.0000000002770707 | 3.0000000405 | 0.0000000405 |
| 9 | 4.0000000000928759 | 4.0000000218 | 0.0000000218 |
| 10 | 4.0000000000932488 | 4.0000000237 | 0.0000000237 |

# Example: the BVP for 6D Helmholtz Eq. for the cube with rip equal to $\pi$

- nsubint:=3; dim:=6; idegr:=nsubint; nhex:=1;
- 84 = N_1(p)=(p+d)!/d!
- allpoints := 60480 N_A=n N_1(p)=720*84 product of number n of elements and number N_1(p) of function in each of n elements.
- allpoint := 4096 N=4096 number of basis functions
- bdomain(720) := 60480 n=d!=6!=720 is number of elements
- a low part of spectrum of 42 degenerate eigenvalues: 0.183360983479286 e-10 , 1.00023, 1.00034, 1.00034, 1.00034, 1.00034, 1.00034,
  2.04760, 2.04760, 2.04760, 2.04760, 2.04760, 2.04760, 2.04760, 2.04760, 2.04760, 2.07391, 2.08478, 2.08478, 2.08478, 2.08478, 2.08478,
  3.15060, 3.15196, 3.15196, 3.15196, 3.15196, 3.15196, 3.15780, 3.15780, 3.15780, 3.15780, 3.15780, 3.16319, 3.16319, 3.16319, 3.16319, 3.16319, 3.16319, 3.16319, 3.16319, 3.16319
- Calculations was performed in Maple 2x 8-core Xeon E5-2667 v2 3.3 GHz, 512 GB RAM, GPU Tesla 2075.
  memory used=540540.0MB, alloc=1307.5MB, time=9234.46

# The algorithm for calculating the parametric derivatives of eigenfunctions ...

## The generalized eigenvalue problem

$$\mathbf{A}^p\boldsymbol{\Phi}^h = \varepsilon^h\mathbf{B}^p\boldsymbol{\Phi}^h, \qquad \left(\boldsymbol{\Phi}^h\right)^T\mathbf{B}^p\boldsymbol{\Phi}^h = 1.$$

## The linear system of inhomogeneous algebraic equations w.r.to the unknown $\partial\boldsymbol{\Phi}^h/\partial z$

$$\mathbf{L}\frac{\partial\boldsymbol{\Phi}^h}{\partial z} \equiv (\mathbf{A}^p - \varepsilon^h\mathbf{B}^p)\frac{\partial\boldsymbol{\Phi}^h}{\partial z} = b \equiv -\left(\frac{\partial\mathbf{A}^p}{\partial z} - \frac{\partial\varepsilon^h}{\partial z}\mathbf{B}^p\right)\boldsymbol{\Phi}^h.$$

$$\left(\frac{\partial\boldsymbol{\Phi}^h}{\partial z}\right)^T\mathbf{B}^p\boldsymbol{\Phi}^h = 0,$$

$$\frac{\partial\varepsilon^h}{\partial z} = \left(\boldsymbol{\Phi}^h\right)^T\frac{\partial\mathbf{A}^p}{\partial z}\boldsymbol{\Phi}^h.$$

## Step k1. Calculate the solutions $\mathbf{v}$ and $\mathbf{w}$ of the auxiliary inhomogeneous systems of algebraic equations with the non-degenerate matrix $\bar{\mathbf{L}}$

$$\bar{\mathbf{L}}\mathbf{v} = \bar{\mathbf{b}}, \quad \bar{\mathbf{L}}\mathbf{w} = \mathbf{d}, \quad \bar{L}_{ss'} = \begin{cases} L_{ss'}, & (s-S)(s'-S) \neq 0, \\ \delta_{ss'}, & (s-S)(s'-S) = 0, \end{cases}$$

$$\bar{b}_s = \begin{cases} b_s, & s \neq S, \\ 0, & s = S, \end{cases} \qquad d_s = \begin{cases} L_{sS}, & s \neq S, \\ 0, & s = S, \end{cases}$$

where $S$ is the number of the element of the vector $\mathbf{B}^p\mathbf{\Phi}^h$ having the greatest absolute value.

## Step k2. Evaluate the coefficient $\gamma$

$$\gamma = -\frac{\gamma_1}{(\mathbf{D}_S - \gamma_2)}, \quad \gamma_1 = \mathbf{v}^T\mathbf{B}^p\mathbf{\Phi}^h, \quad \gamma_2 = \mathbf{w}^T\mathbf{B}^p\mathbf{\Phi}^h, \quad \mathbf{D}_S = (\mathbf{B}^p\mathbf{\Phi}^h)_S.$$

## Step k3. Evaluate the vector $\partial_z\mathbf{\Phi}^h$

$$\frac{\partial\Phi_s^h}{\partial z} = \begin{cases} v_s - \gamma w_s, & s \neq S, \\ \gamma, & s = S. \end{cases}$$

From the above consideration it is evident, that the computed derivative has the same accuracy as the calculated eigenfunction.

The potential matrix elements $H_{ij}^h(z)$ and $Q_{ij}^h(z)$, needed, for example, in Kantorovich reduction, defined as

$$H_{ij}(z)=H_{ji}(z)=\int_\Omega dx g_0(x)\frac{\partial\Phi_i(x;z)}{\partial z}\frac{\partial\Phi_j(x;z)}{\partial z},$$
$$Q_{ij}(z)=-Q_{ji}(z)=-\int_\Omega dx g_0(x)\Phi_i(x;z)\frac{\partial\Phi_j(x;z)}{\partial z}.$$

The potential matrix elements $H_{ij}^h(z)$ and $Q_{ij}^h(z)$ can be calculated using the formulas

$$H_{ij}^h(z)=\left(\frac{\partial\mathbf{\Phi}_i^h}{\partial z}\right)^T\mathbf{B}^p\frac{\partial\mathbf{\Phi}_j^h}{\partial z},\quad Q_{ij}^h(z)=-\left(\mathbf{\Phi}_i^h\right)^T\mathbf{B}^p\frac{\partial\mathbf{\Phi}_j^h}{\partial z}.$$

Let $D(x;z)$ be a continuous and bounded positively defined operator on the space $\mathcal{H}^1$ with the energy norm, $\Phi_i(x,z) \in \mathcal{H}^2$. Then the following estimates for $\varepsilon_i^h(z)$, $\Phi_i^h(x;z) \in \mathcal{H}^1$ are valid [Strang, G., Fix, G.J.: An Analysis of the Finite Element Method. Prentice-Hall, Englewood Cliffs, New York (1973).]

$$\left|\varepsilon_i(z) - \varepsilon_i^h(z)\right| \le c_1 h^{2p}, \quad \left\|\Phi_i(x;z) - \Phi_i^h(x;z)\right\|_0 \le c_2 h^{p+1},$$

$$\|\Phi_i(x;z)\|_0^2 = \int_{\Omega_x} dx g_0(x)\Phi_i(x;z)\Phi_i(x;z),$$

where $h$ is the largest distance between any two points in $\Delta_q$, $p$ is the order of the finite elements, $i$ is the number of the corresponding solutions, and the constants $c_*$ are independent of the step $h$.

Also let $\partial_z U(x;z)$ be continuous and bounded for each value of the parameter $z$, and $\partial_z \Phi_i(x;z) \in \mathcal{H}^2$. Then the following estimates for $\partial_z \varepsilon_i^h(z)$, $\partial_z \Phi_i^h(x;z) \in \mathcal{H}^1$, $H_{ij}^h(z)$, $Q_{ij}^h(z)$) are valid:

$$\left|\frac{\partial \varepsilon_i(z)}{\partial z} - \frac{\partial \varepsilon_i^h(z)}{\partial z}\right| \le c_3 h^{2p}, \quad \left\|\frac{\partial \Phi_i(x;z)}{\partial z} - \frac{\partial \Phi_i^h(x;z)}{\partial z}\right\|_0 \le c_4 h^{p+1},$$

$$\left|Q_{ij}(z) - Q_{ij}^h(z)\right| \le c_5 h^{2p}, \quad \left|H_{ij}(z) - H_{ij}^h(z)\right| \le c_6 h^{2p}.$$

# Example: model of a Helium atom

## The parametric 2D BVP for model of a Helium atom

$$\left[-\frac{\partial}{\partial\lambda}\lambda(1-\lambda)^2\frac{\partial}{\partial\lambda}-\frac{\partial}{\partial\eta}(1-\eta^2)\frac{\partial}{\partial\eta}+\sqrt{2}R(1-\lambda)\frac{(1+\lambda)^2-(1-\lambda)^2\eta^2-8(1-\lambda^2)}{\sqrt{(1+\lambda)^2+(1-\lambda)^2\eta^2}^3}\right.$$
$$\left.+1-\lambda-\varepsilon_i(R)(1-\lambda)^2\frac{(1+\lambda)^2-(1-\lambda)^2\eta^2}{((1+\lambda)^2+(1-\lambda)^2\eta^2)^2}\right]p_i(\lambda,\eta;R)=0.$$

## The boundary and normalization conditions

$$\lim_{\lambda\to 0,1}\lambda(1-\lambda)\frac{\partial p_i(\lambda,\eta;R)}{\partial\lambda}=0,\quad \lim_{\eta\to\pm 1}(1-\eta^2)\frac{\partial p_i(\lambda,\eta;R)}{\partial\eta}=0,$$
$$\frac{1}{2}\int_0^1 d\lambda\int_{-1}^1 d\eta(1-\lambda)^2\frac{(1+\lambda)^2-(1-\lambda)^2\eta^2}{((1+\lambda)^2+(1-\lambda)^2\eta^2)^2}p_i^2(\lambda,\eta;R)=1.$$

The calculations were carried out using the server 2x4 kernels i7k (i7-3770K 4.5 GHz, 32 GB RAM, GPU GTX680), and the Intel Fortran compiler 17.0. The computing time for the considered examples with $10^{-12}$ accuracy on the uniform grids $\lambda=\{0(L)1\}$, $\eta=\{0(L)1\}$ at $L=10,20,40$ is 0.38, 5.08 and 41.21 seconds, respectively.

# Example: model of a Helium atom

The eigenfunction $p_1(\lambda, \eta; R)$ and its parametric derivative $\partial_R p_1(\lambda, \eta; R)$ at $R = 7.65$.

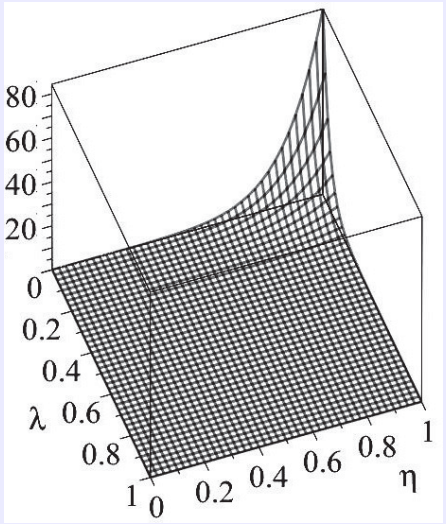


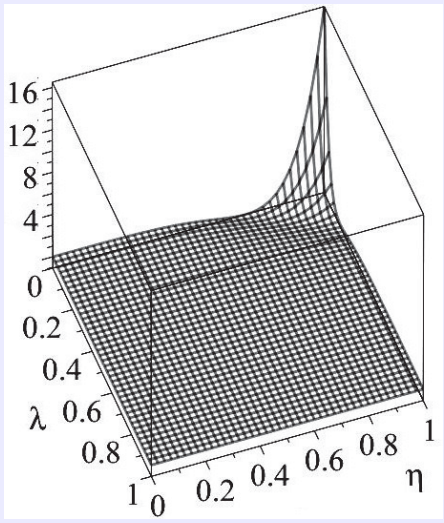


The eigenfunction $p_4(\lambda, \eta; R)$ and its parametric derivative $\partial_R p_4(\lambda, \eta; R)$ at $R = 7.65$.

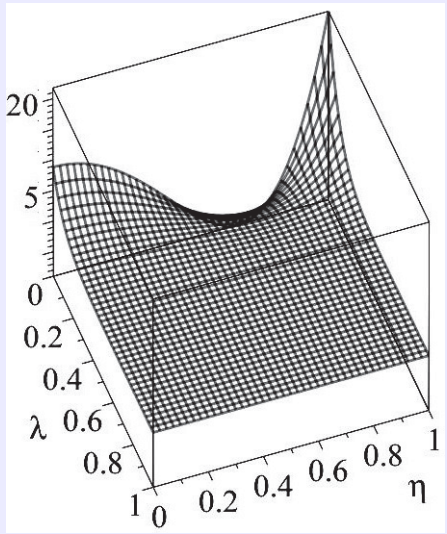


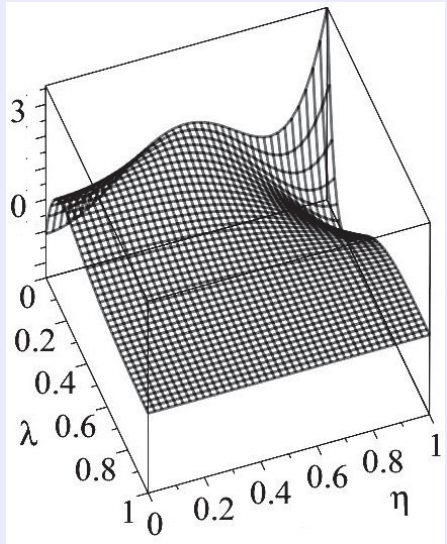

# Example: model of a Helium atom

Comparison of the transformed potential curves $E_j(R) = (\varepsilon_j(R) - 3)/4$ their first derivative by parameter $R$ with results $*$ at $j_{max} = 12$. The mesh points are $\lambda = \{0(L)1\}$ and $\eta = \{0(L)1\}$, and $R = 7.65$ a.u..

| $j$ | $E_j(R)$ $(L = 10)$ | $E_j(R)$ $(L = 20)$ | $E_j(R)$ $(L = 40)$ | $E_j(R)$ $*$ |
|---|---|---|---|---|
| 1 | -63.498 825 358 | -63.499 151 482 | -63.499 153 248 | -63.499 153 256 |
| 2 | -21.451 886 770 | -21.451 891 369 | -21.451 891 391 | -21.451 886 907 |
| 3 | -19.082 401 572 | -19.082 406 568 | -19.082 406 592 | -19.082 325 834 |
| 4 | -13.371 479 034 | -13.371 481 948 | -13.371 481 961 | -13.371 480 623 |
| 5 | -11.876 674 062 | -11.876 679 657 | -11.876 679 683 | -11.876 677 566 |
| 6 | -8.898 971 861 | -8.898 980 996 | -8.898 981 042 | -8.897 839 854 |
| $j$ | $\partial_R E_j(R)$ $(L = 10)$ | $\partial_R E_j(R)$ $(L = 20)$ | $\partial_R E_j(R)$ $(L = 40)$ | $\partial_R E_j(R)$ $*$ |
| 1 | -15.795 727 590 | -15.796 133 881 | -15.796 136 178 | -15.796 136 189 |
| 2 | -3.997 423 220 | -3.997 429 139 | -3.997 429 168 | -3.997 431 891 |
| 3 | -4.142 653 692 | -4.142 660 186 | -4.142 660 217 | -4.142 711 985 |
| 4 | -3.897 819 472 | -3.897 822 446 | -3.897 822 460 | -3.897 824 374 |
| 5 | -3.314 361 245 | -3.314 363 641 | -3.314 363 652 | -3.314 347 679 |
| 6 | -2.705 442 515 | -2.705 445 914 | -2.705 445 931 | -2.705 544 197 |

$*$ Gusev, A.A., Chuluunbaatar, O., Vinitsky ,S.I., and Abrashkevich, A.G., "POTHEA: a program for computing eigenvalues and eigenfunctions and their first derivatives with respect to the parameter of the parametric self-adjoined 2D elliptic partial differential equation," Comput. Phys. Commun. 185 (10), 2636–2654 (2014).

## Resume

- High-accuracy finite element method for solving the 2D parametric elliptic self-adjoint boundary-value problems is presented.
- The triangular elements and new high-order fully symmetric Gaussian quadratures with positive weights, and no points are outside the triangle (PI type) is applied. The program calculates with the given accuracy the eigenvalues, the surface eigenfunctions and their first derivatives with respect to the parameter of the BVP for parametric self-adjoint elliptic differential equation with the mixed Dirichlet-Neumann type boundary conditions on the 2D polygonal domain, and the potential matrix elements, expressed as integrals of the products of surface eigenfunctions and/or their first derivatives with respect to the parameter.
- We demonstrated an efficiency of finite element schemes and program by means of benchmark calculations the 3D boundary-value problem for Helium atom bound states in the framework of Kantorovich method.

Thank you for your attention